Magnetic nanographite

Koichi Kusakabe* and Masanori Maruyama†
Graduate School of Science and Technology, Niigata University, Ikarashi, Niigata 950-2181, Japan
(Received 2 October 2002; revised manuscript received 11 December 2002; published 28 March 2003)

Hydrogenated nanographite can display spontaneous magnetism. Recently, we proposed that hydrogenation of nanographite is able to induce finite magnetization. We have performed theoretical investigation of a graphene ribbon, in which each carbon is bonded to two hydrogen atoms at one edge and to a single hydrogen atom at another edge. Application of the local-spin-density approximation to the calculation of the electronic band structure of the ribbon shows the appearance of a spin-polarized flat band at the Fermi energy. Producing different numbers of monohydrogenated carbons and dihydrogenated carbons can create magnetic moments in nanographite.

DOI: 10.1103/PhysRevB.67.092406 PACS number(s): 75.75.+a, 75.50.Xx, 73.20.At, 73.22.−f

Recent reports on magnetic carbon have stimulated renewed interest in carbon systems as possible new magnetic materials made exclusively of light elements. These investigations include experiments suggesting ferromagnetic behavior in polymerized fullerenes made using photoassisted oxidation[1] or high-pressure treatment.[2] A nanometer-scale graphite called nanographite may yield another magnetic carbon system. Some experiments have demonstrated the existence of anomalous magnetic behavior unexpected in diamagnetic bulk graphite.[3–5]

Several theoretical investigations of nanographite have been carried out prior to or parallel to these experiments.[6–14] An important finding was that π electrons in nanometer-scale graphite are strongly affected by structure of edges. A typical edge is the zigzag edge. The zigzag edge was found in STM images of nanometer scale graphene,[15,16] although the armchair edge has lower energy than the zigzag edge.[17,18] Fujita and co-workers suggested that the π electrons on a monohydrogenated zigzag edge may create a ferrimagnetic spin structure on the edge.[6] Magnetism with localized-spin moments is possible due to the existence of nonbonding localized states at the zigzag edge. These states are called edge states and are highly degenerate at the Fermi level and may be spin polarized. Such an edge state does not appear on an armchair edge. Klein has studied another edge of graphene strips, considering a zigzag edge with an atomic site having a π orbital on the edge.[19,20] Examining a tight-binding model of π electrons, he found degenerate surface states on the edge, which is referred to here as a bearded edge.

The total spin moment of a graphene ribbon, however, should be zero, if both of the two edges of the ribbon are zigzag edges, or if both of them are bearded edges. This is because, the structure of the π network becomes a bipartite lattice having the same number of sublattice sites. In such cases, an argument using the Hubbard model results in zero spin moment, following the Lieb theorem.[6,21] Naively, we may say that local magnetic moments at the two edges are coupled antiferromagnetically.[6]

In this Brief Report, we show that a hydrogenated graphene ribbon can have a finite total magnetic moment. A key point is the structure of the two edges of the ribbon. In our ribbon, one of the edges is composed of monohydrogenated carbon atoms and another is made of dihydrogenated ones. By a first-principles electronic-state calculation, we will show that the system is stable and has a fully spin-polarized flat band. A finite spontaneous magnetization appears in the graphene ribbon.

We present here our idea to find magnetic nanographite. If a graphene ribbon has a bearded edge on one side and a zigzag edge on the other side, the π network becomes a bipartite lattice with different numbers of sublattice sites.[22,23] Then, a flat band appears at the Fermi level. The band is fully spin polarized if interelectron interactions e.g. the Hubbard repulsion U is considered.[21] In addition, the flat band consists of edge states, so that the magnetic moments are localized at both edges and the distribution of moments shows exponential decay in the π network.[23] However, to design a realistic material, we also have to specify the atomic configuration of the bearded edge.

We found that one solution is a zigzag edge whose end carbon atoms are dihydrogenated.[24] In order to present an example of magnetic nanographite, we will show the electronic band structure of the ribbon which has a completely spin-polarized flat band at the Fermi energy. The magnetism will be explained using a Hubbard model.

To investigate the stability and magnetic structure of the nanographite, we used an electronic-state calculation with a local-spin-density approximation (LSDA) based on the density-functional theory.[25,26] An LSDA functional given by Perdew and Wang[27] was utilized as the exchange-correlation energy functional. The ultrasoft pseudopotential generated using the Vanderbilt strategy was adopted.[28] The valence wave functions were expanded in a plane-wave basis set. To achieve convergence in the total energy, we used an energy cutoff E_c of 49 Ry for structural optimization in a fixed unit cell. To reduce computation time, we adopted $E_c = 25$ Ry to optimize the size of the unit cell before the final optimization of inner coordinates. Structural optimization was performed until each component of the interatomic force became less than 8×10^{-5} H/a.u. The calculations were done using a computer program called the Tokyo *ab initio* program package (TAPP).[29]

To check the accuracy of our calculation, we obtained the structural parameters of a hydrogen molecule, a CH_4 molecule, a C_2H_4 molecule, diamond and graphite. The bond length of each molecule and the bond angles of CH_4 and

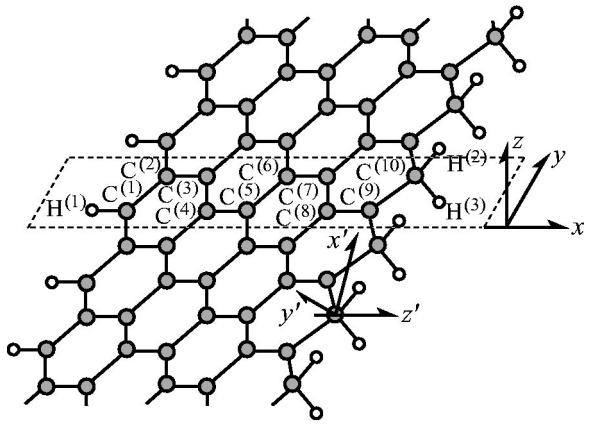

FIG. 1. A structural model of a magnetic graphene ribbon. Dark circles represent carbon atoms and open circles denote hydrogen atoms. Dashed lines represent a section of a unit cell in the x-y plane. The unit cell contains $2n$ carbon atoms and three hydrogen atoms. Here a case with $n=5$ is shown. Two sets of three-dimensional coordinate axes, (xyz) and $(x'y'z')$, are displayed. The x axis and the y axis are in a graphene plane. Three axes x', y', and z' point to the (011), (0-11), (100) directions, respectively, in the (xyz) coordinate.

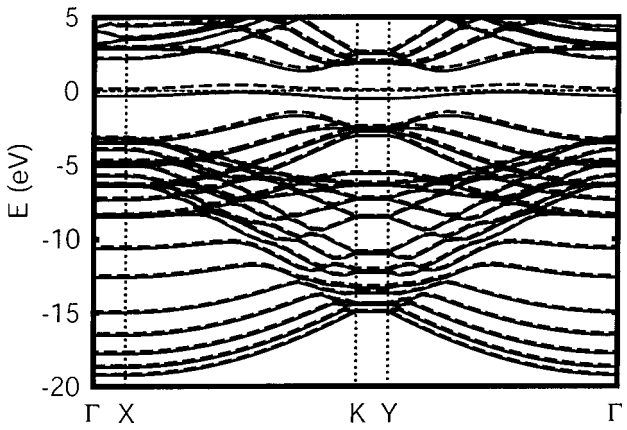

FIG. 2. The electronic band structure of a hydrogenated graphene ribbon. Solid lines and dashed lines represent the dispersion relation of bands for up electrons and down electrons, respectively. At the Fermi level $E_F=0$, a dispersionless band appears. The band is completely spin polarized. Above and blow the flat band, there are eight π bands, which are from the 18th band to the 21st band and from the 23rd band to the 26th band on the K-Y line. The 17th band on the K-Y line is composed mainly of $1s$ orbitals of two hydrogen atoms $H^{(2)}$ and $H^{(3)}$ in Fig. 1.

C_2H_4 were obtained with relative errors less than 3.3%. The vibrational energy $\hbar\omega_e$ of H_2 was 1.92×10^{-2} [H], which is about 4% smaller than 2.00×10^{-2} [H] observed. For cubic diamond, the lattice constant, the bulk modulus, and its pressure derivative were 6.677 a.u., 4.66 Mbar, and 3.68. For hexagonal graphite, the lattice constants were $a=4.616$ a.u. and $c=12.67$ a.u. These values are in reasonable agreement with the values determined experimentally or by previous calculations.[30] Band structures of the solids also reproduced previous results.[30]

Consider the graphene ribbon shown in Fig. 1. In this structure, each dark circle represents the position of a carbon atom. Solid lines represent σ bonds. Each open circle is a hydrogen atom. For convenience, we number atoms and name them $C^{(1)}\cdots C^{(2n)}$ and $H^{(1)}\cdots H^{(3)}$ in a unit cell. Here, n is a positive integer. On the left edge, each carbon atom is bonded to a hydrogen atom and has a π orbital. On the right edge, each carbon atom has bonds to two hydrogen atoms and two neighboring carbon atoms. If we consider that the dihidrogenated carbon atom $C^{(2n)}$ forms sp^3 bonds instead of sp^2 bonds, $C^{(2n)}$ loses a π electron. Since there remain $2n-1$ carbon atoms having a π electron per each in a unit cell, the π network might become a bipartite lattice with different numbers of sublattice sites.

We can consider ribbons with various widths. However, we know that the optimum width is given by $n\simeq5\sim10$ for nanographite ribbons with zigzag edges.[7] In any case, the essential properties should be the same irrespective of the width. Thus we first consider a ribbon with $n=5$ and discuss dependence of magnetism on the width of the graphene ribbon at the end of the paper.

To examine our idea, we have performed an LSDA calculation. Below, we assume a periodic boundary condition. Since the structure is one dimensional, we are allowed to use k points along the y axis as $(0,k_y,0)$ for the structural optimization. We used 6 k points uniformly distributed in the Brillouin zone for most simulations. We determined the equilibrium lattice constant of the ribbon, which became 4.674 a.u. For the calculation to optimize the inner parameters, the size of the cell was taken to be $40.27\times4.647\times18.60$ $(\text{a.u.})^3$. The spacing between neighboring ribbons became 19.5 a.u. in the x direction and 15.3 a.u. in the z direction. The structure was optimized by a conjugate gradient method. The obtained results did not change when we used 12 k points instead. The bond length of C-C ranged from about $2.64\sim2.70$ a.u. for neighboring carbon pairs except for 2.59 a.u. between $C^{(8)}$ and $C^{(9)}$ and 2.76 a.u. between $C^{(9)}$ and $C^{(10)}$. Bond angles $H^{(2)}$-$C^{(10)}$-$H^{(3)}$ and $C^{(9)}$-$C^{(10)}$-$C^{(9)}$ are 100.7° and 114.8°. These structure parameters suggest that the end carbon $C^{(10)}$ forms sp^3 bonds.

An electronic band structure of the graphene ribbon is shown in Fig. 2. In the first Brillouin zone, the Γ-Y line corresponds to a one-dimensional axis on which a k vector is parallel to the ribbon. A flat band appears at the Fermi level. The band is almost dispersionless in the whole Brillouin zone and is completely spin polarized. That is, only the spin-up branch is filled and the spin-down branch is empty. Splitting between polarized flat bands for up electrons and down electrons is approximately $0.5\sim0.6$ eV and the gap between them is ~0.2 eV. These values give a rough energy scale of stiffness for the magnetic ground state. The total spin S_{tot} becomes 1/2 times number of unit cells N_c. Stability of the polarized flat band was confirmed by using a unit cell which was doubled in the y direction.

The flat band is the center band of nine well-characterized π bands. See band dispersion around the Y point in Fig. 2. The dispersion relation of these π bands is roughly the same as those obtained for a simple tight-binding model with nine π orbitals on a graphene ribbon. In Fig. 2, all branches for up electrons and down electrons are split by spin polarization.

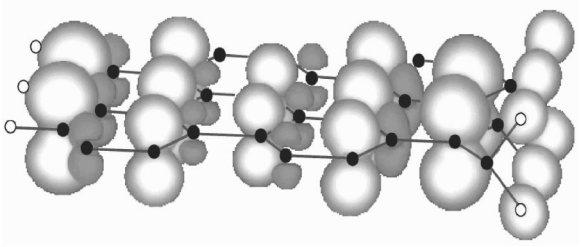

FIG. 3. The optimized structure of a magnetic graphene ribbon. Closed spheres and open spheres represent the positions of carbon atoms and hydrogen atoms, respectively. Spin density on the ribbon is displayed by isosurfaces. Bright surfaces and dark surfaces represent spin-up density and spin-down density. The isolevel is set to 1/4 of the maximum amplitude of the spin-up density.

This result implies that a magnetic moment appears on every atom. We show obtained spin density in Fig. 3. A ferrimagnetic spin structure is clearly seen. A local spin moment exists on every carbon atom. Interestingly, finite spin moments appear on two hydrogen atoms which have bondings with $C^{(10)}$. The reason will be explained below. Thus, the graphene ribbon is confirmed to be magnetic in the LSDA model. We call this structure magnetic nanographite.

We found a curious characteristic of the wave functions of the flat band. We surmise that only nine carbon atoms in the unit cell possess π orbitals which contribute to the π bands. This is because sp^3 bonds are created at the dihydrogenated carbon atom $C^{(10)}$. Wave functions on the flat band were nonbonding edge states with finite amplitude on only odd-numbered carbon atoms, but not on even-numbered ones. An interesting point is that a finite amplitude was found on two hydrogen atoms $H^{(2)}$ and $H^{(3)}$. Therefore, we have to consider $1s$ orbitals on these hydrogen atoms in order to analyze the spin-polarized flat band.

Let us introduce two sets of orthogonal coordinates, (xyz) and $(x'y'z')$ as defined in Fig. 1. Four sp^3 orbitals on $C^{(10)}$ may be represented as $\phi_1=\phi_s+\phi_{x'}+\phi_{y'}+\phi_{z'}$, $\phi_2=\phi_s-\phi_{x'}-\phi_{y'}+\phi_{z'}$, $\phi_3=\phi_s+\phi_{x'}-\phi_{y'}-\phi_{z'}$, and $\phi_4=\phi_s-\phi_{x'}+\phi_{y'}-\phi_{z'}$. Here, ϕ_s is a $2s$ orbital and ϕ_m $(m=x',y',z')$ are three $2p$ orbitals on $C^{(10)}$. ϕ_1 and ϕ_2 point to $H^{(2)}$ and $H^{(3)}$, respectively. We take linear combinations of ϕ_1 and ϕ_2 as well as $1s$ orbitals φ_1 and φ_2 on $H^{(2)}$ and $H^{(3)}$ and define $\overline{\phi}_\pm=(\phi_1\pm\phi_2)/\sqrt{2}$ and $\overline{\varphi}_\pm=(\varphi_1\pm\varphi_2)/\sqrt{2}$. Note that $\overline{\phi}_-=\phi_z$, i.e. a π orbital on $C^{(10)}$. By symmetry, $\overline{\phi}_-$ and $\overline{\varphi}_-$ hybridize with the π orbitals of the host π system of the graphene sheet, but not with σ orbitals in the honeycomb lattice. Therefore, we must utilize $\overline{\phi}_-$ and $\overline{\varphi}_-$ as well as the π orbitals on $C^{(i)}$ $(i=1,\cdots 9)$ to analyze the π network in the magnetic nanographite.

If we adopt the above representation, we obtain an effective model describing the ribbon. The model consists of 11 local orbitals in a unit cell. Here we ignore overlap integrals between orbitals for simplicity. Introducing the operator representation $c_{i,\sigma}$ for a π electron on a carbon atom and $d_{l,\sigma}$ for an electron in $\overline{\varphi}_-$ in the lth unit cell, we obtain an effective Hamiltonian

$$H=-\sum_{\langle i,j\rangle}\sum_{\sigma} t_{i,j}(c^{\dagger}_{i,\sigma}c_{j,\sigma}+\text{H.c.})+\sum_{i} Un_{i,\uparrow}n_{i,\downarrow}$$
$$-\sum_{\langle i,l\rangle}\sum_{\sigma} t'_{i,l}(c^{\dagger}_{i,\sigma}d_{l,\sigma}+\text{H.c.})+\sum_{l} U'm_{l,\uparrow}m_{l,\downarrow}$$
$$+\varepsilon\sum_{l}\sum_{\sigma} m_{l,\sigma}. \quad (1)$$

Here, an index i specifying a carbon atom runs over all carbon sites. Two kinds of number operators are defined as $n_{i,\sigma}\equiv c^{\dagger}_{i,\sigma}c_{i,\sigma}$ and $m_{l,\sigma}\equiv d^{\dagger}_{l,\sigma}d_{l,\sigma}$. Bond connections given by nonzero $t_{i,j}$ and $t'_{i,l}$ are the same as those in a graphene ribbon with a zigzag edge and a bearded edge.[23] We set the origin of the energy at the orbital energy of the $2p$ orbital ε_{2p} on carbon. ε_{1s} denotes the energy of a $1s$ electron on a hydrogen atom and ε is given by $\varepsilon=\varepsilon_{1s}-\varepsilon_{2p}$. Since $\varepsilon<0$, a band mainly composed of $\overline{\varphi}_-$ is separated in energy from other π bands. This property is also seen in the LSDA band structure, where the 17th band on the K-Y line in Fig. 2 is the corresponding band.

Consider a periodic boundary condition for a finite system with N_c unit cells. If $\varepsilon=0$ and if $U'=U$, Lieb's theorem is applicable and the ground state becomes a ferrimagnetic state with a total magnetization $S_{\text{tot}}=|N_A-N_B|/2$. Here the difference in sublattice sites $|N_A-N_B|$ equals N_c. This magnetic ground state is thought to be stable against perturbation like $\varepsilon<0$, since (1) there is a finite gap between the flat band and other π bands both in the tight-binding description and in the LSDA result in Fig. 2, (2) we have confirmed that a small difference of ε_{1s} and ε_{2p} does not break the flatness of the center band in the tight-binding model. Thus the magnetism found in an LSDA calculation can be understood as the appearance of ferrimagnetism in a flat-band Hubbard model.

The formation energy of a dihydrogenated edge has been evaluated by comparing the total energy within LSDA. We denote E_{H_2}, E_{G1}, and E_{G2} as the energy of a hydrogen molecule, that of a graphene ribbon with monohydrogenated zigzag edges and that of a magnetic nanographite ribbon, respectively. The latter two are energy per a unit cell including $2n$ carbon atoms. Our calculation shows that $E_{G2}-(E_{G1}+E_{H_2}/2)\simeq 0.3$ eV for $n=5$. Thus, the hydrogenation of nanographite with monohydrogenated zigzag edges is confirmed to be an endothermic reaction. Utilization of proper catalysts in catalytic reduction may be important in the synthesis of magnetic nanographite.

To see how our conclusion is affected by changing the width of the ribbon, we performed the LSDA calculation for ribbons with a width from $n=2$ to $n=4$. A ferrimagnetic structure was found even in these narrow ribbons. These ribbons do not show the Peierls distortion, which is similar to conclusions on the monohydrogenated zigzag ribbons.[8,10,31]

We have shown that a spin-polarized flat band appears in the LSDA band structure of a graphene ribbon. The origin of the magnetism is explained as a realization of the flat-band ferromagnetism. An orbital $\overline{\varphi}_-$ on two hydrogen atoms $H^{(2)}$ and $H^{(3)}$ is an antibonding orbital and has symmetry p_z.

Thus, hydrogenation of a carbon atom is identified as the addition of a π orbital at a zigzag edge. The structure may be regarded as a realization of the bearded edge. We can expect magnetism for any hydrogenated ribbon with $|N_A - N_B| > 0$, even if dihydrogenation of the zigzag edge is not perfect. The same effect is also expected with fluorination.[32] In this Brief Report we have considered a ribbon with a flat graphene structure, but the method is also applicable to nanotubes with zigzag edges. Thus it appears that, a magnetic nanotube may be designed.[24]

One of the authors K.K. is grateful for fruitful discussions with Professor T. Enoki and Dr. Takai. This work was supported by a Grant-in-Aid from the Ministry of Education, Culture, Sports, Science and Technology of Japan. The calculation was partly performed at the computer facility of ISSP, University of Tokyo.

*Electronic address: kabe@sunshine.gs.niigata-u.ac.jp
†Electronic address: maruyama@sunshine.gs.niigata-u.ac.jp

[1] Y. Murakami and H. Suematsu, Pure Appl. Chem. **68**, 1463 (1996).
[2] T.L. Makarova, B. Sundqvist, R. Hohne, P. Esquinazi, Y. Kopelevich, P. Scharff, V.A. Davydov, L.S. Kashevarova, and A.V. Rakhmanina, Nature (London) **413**, 716 (2001).
[3] Y. Shibayama, H. Sato, T. Enoki, and M. Endo, Phys. Rev. Lett. **84**, 1744 (2000).
[4] B.L.V. Prasad, H. Sato, T. Enoki, Y. Hishiyama, Y. Kaburagi, A.M. Rao, P.C. Eklund, K. Oshida, and M. Endo, Phys. Rev. B **62**, 11 209 (2000).
[5] Y. Kopelevich, P. Esquinazi, J.H.S. Torres, and S. Moehlecke, J. Low Temp. Phys. **119**, 691 (2000).
[6] M. Fujita, K. Wakabayashi, K. Nakada, and K. Kusakabe, J. Phys. Soc. Jpn. **65**, 1920 (1996).
[7] K. Nakada, M. Fujita, G. Dresselhaus, and M. Dresselhaus, Phys. Rev. B **54**, 17 954 (1996).
[8] M. Fujita, M. Igami, and K. Nakada, J. Phys. Soc. Jpn. **66**, 1864 (1997).
[9] K. Wakabayashi, M. Sigrist, and M. Fujita, J. Phys. Soc. Jpn. **67**, 2089 (1998).
[10] Y. Miyamoto, K. Nakada, and M. Fujita, Phys. Rev. B **59**, 9858 (1999).
[11] K. Harigaya, J. Phys.: Condens. Matter **13**, 1295 (2001).
[12] K. Harigaya, Chem. Phys. Lett. **340**, 123 (2001).
[13] S. Okada and A. Oshiyama, Phys. Rev. Lett. **87**, 146803 (2001).
[14] K. Harigaya and T. Enoki, Chem. Phys. Lett. **351**, 128 (2002).
[15] T. Land, T. Micherly, R. Behm, J. Hemminger, and G. Comsa, Surf. Sci. **264**, 261 (1992).
[16] A. Nagashima, H. Itoh, T. Ichinokawa, C. Oshima, and S. Otani, Phys. Rev. B **50**, 4756 (1994).
[17] A. Thess *et al.*, Science **273**, 483 (1996).
[18] Y. Lee, S. Kim, and D. Tománek, Phys. Rev. Lett. **78**, 2393 (1997).
[19] D.J. Klein, Chem. Phys. Lett. **217**, 261 (1994).
[20] D.J. Klein and L. Bytautas, J. Phys. Chem. A **103**, 5196 (1999).
[21] E. Lieb, Phys. Rev. Lett. **62**, 1201 (1989).
[22] K. Wakabayashi and M. Sigrist, Phys. Rev. Lett. **84**, 3390 (2000).
[23] K. Kusakabe and Y. Takagi, Mol. Cryst. Liq. Cryst. **387**, 231 (2002).
[24] K. Kusakabe and M. Maruyama, Tanso **205**, 238 (2002).
[25] P. Hohenberg and W. Kohn, Phys. Rev. **136**, B864 (1964).
[26] W. Kohn and L. Sham, Phys. Rev. **140**, A1133 (1965).
[27] J.P. Perdew and Y. Wang, Phys. Rev. B **45**, 13 244 (1992).
[28] D. Vanderbilt, Phys. Rev. B **41**, 7892 (1990).
[29] J. Yamauchi, M. Tsukada, S. Watanabe, and O. Sugino, Phys. Rev. B **54**, 5586 (1996).
[30] J. Furthmuller, J. Hafner, and G. Kresse, Phys. Rev. B **50**, 15 606 (1994).
[31] M. Kertesz and R. Hoffmann, Solid State Commun. **47**, 97 (1983).
[32] M. Maruyama and K. Kusakabe (unpublished).